

# Robot-guided eddy current measurement of yarn orientation change during stepwise 3D draping

G Bardl<sup>1</sup>, A M Khan<sup>1</sup>, A Nocke<sup>1</sup> and C Cherif<sup>1</sup>

<sup>1</sup> Institute of Textile Machinery and High Performance Material Technology, Technical University Dresden, Germany

Email: georg.bardl@tu-dresden.de

**Abstract.** The production of high-performance carbon fiber-reinforced plastics (CFRP) involves the draping of the carbon fiber fabrics to a 3D shape, a process which changes the orientation of the load-bearing fibers in the fabric and therefore has a high impact on the strength of the final composite part. This paper investigates the change in yarn orientation during the 3D-draping process of biaxial carbon-fiber non-crimp fabrics to a hemispherical shape. The draping process is partitioned in several steps, after each of which the yarn orientation in the fabric is measured by a robot-guided eddy current scanning system. The results show that the greatest change in yarn orientation occurs in the final stages of the draping. Furthermore, the yarn orientation change is not linear – in some regions, later draping steps reverse the yarn orientation change from earlier steps. These results are of high importance for a better controlling of the textile draping process.

## 1. Introduction

When draping textile fabrics to three-dimensional shapes, the main deformation mechanism is the shearing of the fabrics, which results in a change of the yarn orientation. For the manufacturing of fiber-reinforced plastics, where the fibers carry the mechanical loads in the composite, knowledge of the yarn orientation after draping is crucial in order to assess the composite's mechanical strength. Although optical methods [1–3] provide a fast and reliable way to assess the fiber orientation, they are limited to the upper fabric layer. If the inspection of deeper, optically non-visible layers is desired, electromagnetic inspection methods like eddy current testing can be applied [4–7]. In eddy current testing, a sensor with an emitter and a receiver coil is moved over the surface of the conductive specimen. Since the electric properties of the specimen influence the impedance of the receiver coil, an image of the local electrical properties is generated. Figure 1 shows an example eddy current scan result for a biaxial  $\pm 45^\circ$  fabric. Notice that individual yarns of both the upper and the lower, optically non-visible layer, can be distinguished.

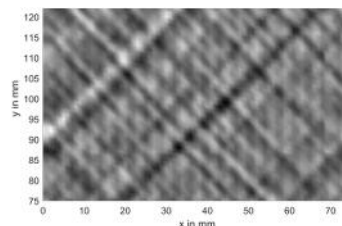


**Figure 1.** Eddy current scan of a  $\pm 45^\circ$  non-crimp fabric.



From the eddy current scan image, the yarn direction of the individual layers can be determined by a 2D Fourier Transform method [8], a technique which has been extended to 3D draped fabrics recently [7]. The aim of the presented research is to use this method to investigate the progressive change in yarn orientation which occurs during the textile draping process. Therefore, the textile draping experiment with a hemispherical punch is partitioned into several steps, after each of which the yarn orientation is measured by a robot-guided eddy current scanning system.

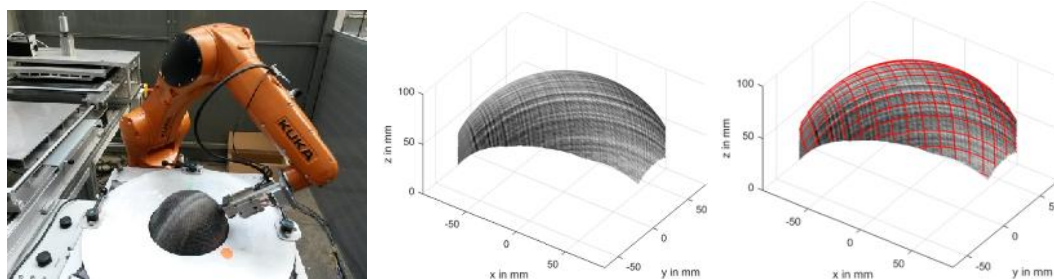
## 2. Materials and methods

Table 1 shows the specifications of the used carbon fiber non-crimp fabrics. The fabrics are biaxial ( $\pm 45^\circ$ ) and were produced on a Malimo 14024 stitch-bonding machine.

**Table 1.** Non-crimp fabric specification.

	Orientation in $^\circ$	Area weight in $\text{g/m}^2$	Fiber
Layer 1	-45	222	Toho Tenax HTS45-E23 800 tex
Layer 2	+45	222	Toho Tenax HTS45-E23 800 tex
Stitching	Tricot	13	PES-t 7,6 tex

For the draping experiment, a test stand designed by HTS Coswig (Germany) is used, which pushes a hemispherical punch with a radius  $R = 100$  mm through the textile from below. The forming is done in several steps by extending the punch to the heights  $h = 25, 50, 75$  and  $100$  mm consecutively. At  $h = 0$  mm and after each of the four draping steps, the surface is scanned with an eddy-current sensor mounted to an industrial 6-axis robot (Figure 2a). From the 3D eddy current scan results (Figure 2b), the yarn orientations of both the upper and the lower, optically non-visible layer are determined by an automatic algorithm and the paths of individual yarns on the surface are reconstructed (Figure 2c), a process described in detail in [7].



**Figure 2.** Eddy current scanning (left), eddy current scan (center) and evaluated fiber paths (right).

## 3. Results

Figure 3, 4 and 5 show the scanning process, the eddy current result and the detected yarn paths for three example punch heights  $h = 0, 50$  and  $100$  mm.

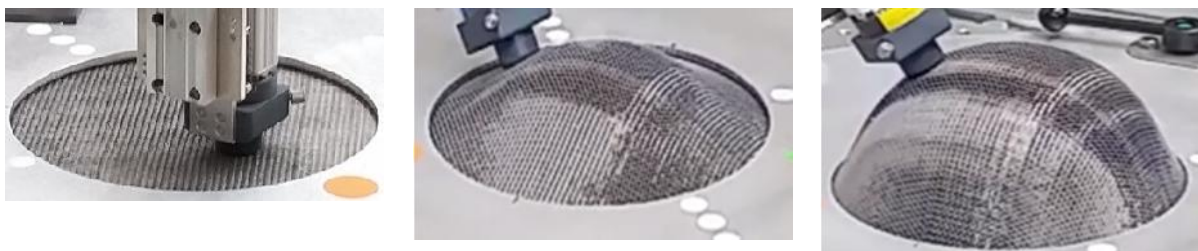


**Figure 3.** Scanning process for punch heights  $h = 0$  mm,  $h = 50$  mm and  $h = 100$  mm (left to right).

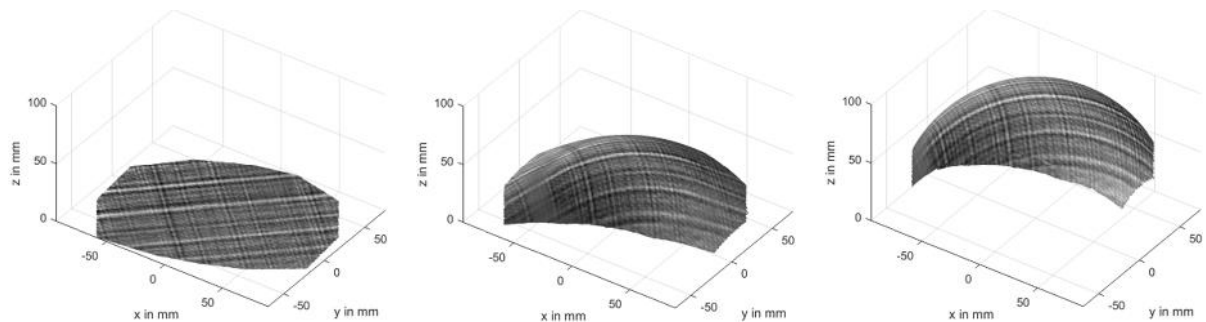


**Figure 4.** Scanning process for punch heights  $h = 0$  mm,  $h = 50$  mm and  $h = 100$  mm (left to right).

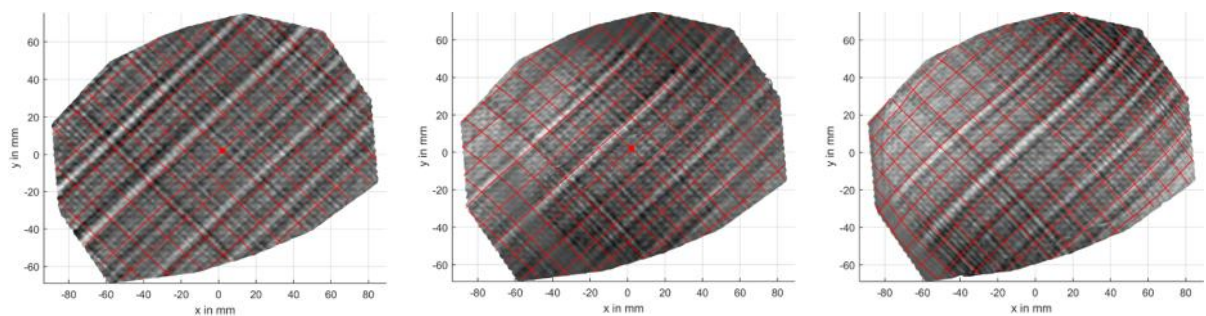


**Figure 5.** Reconstructed yarn paths for punch heights  $h = 0$  mm,  $h = 50$  mm and  $h = 100$  mm.

The extracted yarn paths for all draping steps are overlaid to show the change in yarn orientation for both layers (Figure 6). It can clearly be seen that the greatest yarn orientation change occurs in the outer regions of the hemisphere.

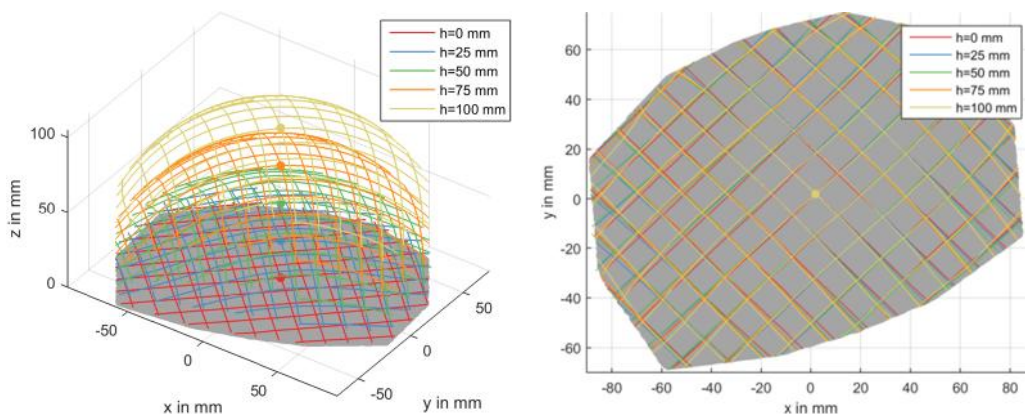


**Figure 6.** Yarn paths at different punch heights.

With the local yarn orientation known before and after each draping step, the change in yarn orientation initiated by each step can be calculated. This is done by segmenting the 3D surface in small areas and, for each area, subtracting the yarn angle after each step from the yarn angle before that step. Figure 7 and 8 show this change in yarn angle for all steps and for both layers. Notice that the yarn angle here is defined as the angle between the vector of the yarn orientation, projected into the  $xy$ -plane, and the vertical line  $y = 0$  mm. Thus, the yarn angle is the angle which would be recorded by an observer who is looking straight down onto the hemisphere.

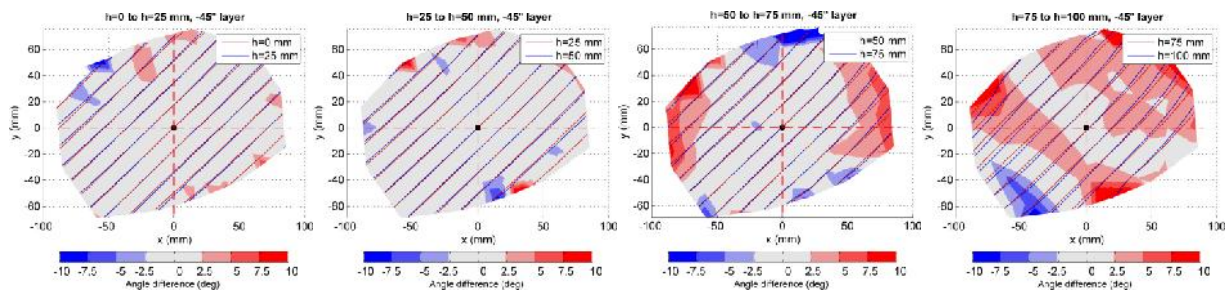


**Figure 7.** Changes in yarn angle for each draping step, top layer ( $-45^\circ$ ).

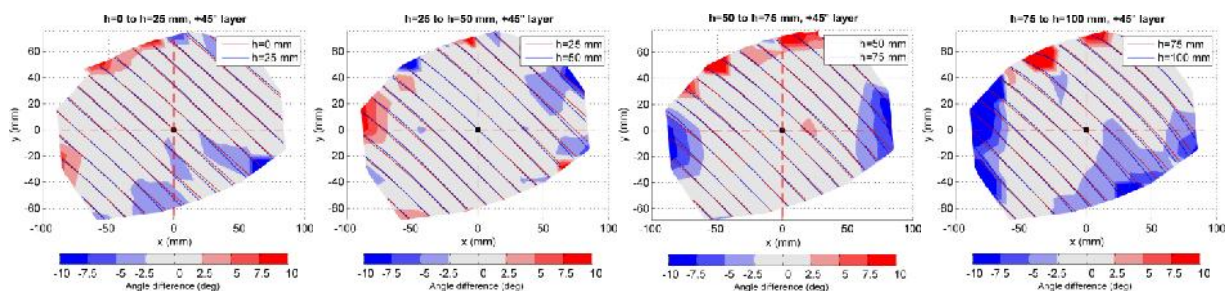


**Figure 8.** Changes in yarn angle for each draping step, bottom layer ( $+45^\circ$ ).

#### 4. Discussion

Several important points can be derived from the analysis of the yarn angle change in each draping step:

1. In this experiment, the greatest change in yarn angle occurs in the last quarter of the forming (from  $h = 75$  to  $h = 100$  mm). This is true for both layers.
2. The absolute changes in yarn angle are higher for the top layer ( $+45^\circ$ )
3. During draping, the yarn angle change in some region reverses its direction: e.g. for the bottom layer ( $+45^\circ$ , Figure 7), the yarn angle in the very left corner increases (red) from 0 to 25 and 50 mm, but decreases (blue) from 50 to 75 and from 75 to 100 mm. The same occurs in the uppermost area for the top layer, which changes from decreasing angle (blue) for the step from  $h = 50$  to 75 mm, to increasing angle (red) in the last step from 75 to 100 mm. This reversal in orientation change can already be seen in the eddy current scans in Figure 4.

The reason for the reversal in yarn orientation change is most likely the formation of wrinkles outside the scan area, which relaxes highly-sheared regions by pushing the material out-of-plane.

#### 5. Conclusion and outlook

This work presented a process to measure the yarn orientation of two-layer non-crimp fabrics automatically with 3D eddy current testing. Measurements were taken before and after each draping step, and yarn paths were reconstructed for each measurement. From these yarn paths, the change in yarn angle was computed for each step. The results show that in the measured zone of the surface, the highest fiber reorientation occurs in the final quarter of the draping, and is unequal between the layers. Some regions reverse the yarn angle change during the draping. These results can serve as an important tool for the validation of draping simulations and for the optimization of the draping process.

Further work will be aimed at using this method for the comparison of the draping performance of different fabric constructions. Also, comparisons with draping simulations will be done to further investigate the process of yarn reorientation during draping.

### Acknowledgments

The IGF research project 18428 BG/1 of the Forschungsvereinigung Forschungskuratorium Textil e. V. is funded through the AiF within the program for supporting the „Industriellen Gemeinschaftsforschung (IGF)“ from funds of the Federal Ministry of Economics and Energy (BMWi) by a resolution of the German Bundestag. The research relating to the robotics engineering was funded by the European Union Regional Development Fund (EFRE) and the Free State of Saxony under grant SAB 100224749. The authors would like to thank the mentioned institutions for providing the funding.

The ITM would like to thank the mentioned institutions for providing financial funds.

### References

- [1] Lomov SV, Boisse P, Deluycker E, Morestin F, Vanclooster K, Vandepitte D, Verpoest I and Willems A 2008 Full-field strain measurements in textile deformability studies *Compos. Part Appl. Sci. Manuf.* **39** 1232–44
- [2] Vanclooster K, Lomov SV and Verpoest I 2009 Experimental validation of forming simulations of fabric reinforced polymers using an unsymmetrical mould configuration *Compos. Part Appl. Sci. Manuf.* **40** 530–9
- [3] Gereke T, Döbrich O, Hübner M and Cherif C 2013 Experimental and Computational Composite Textile Reinforcement Forming: A review *Compos. Part Appl. Sci. Manuf.* **46** 1–10
- [4] Mook G, Lange R and Koeser O 2001 Non-destructive characterisation of carbon-fibre-reinforced plastics by means of eddy-currents *Compos. Sci. Technol.* **61** 865–73
- [5] Schulze MH, Heuer H, Küttner M and Meyendorf N 2010 High-resolution eddy current sensor system for quality assessment of carbon fiber materials *Microsyst. Technol.* **16** 791–7
- [6] Heuer H, Schulze M, Pooch M, et al. 2015 Review on quality assurance along the CFRP value chain – Non-destructive testing of fabrics, preforms and CFRP by HF radio wave techniques *Compos. Part B Eng.* **77** 494–501
- [7] Bardl G, Nocke A, Cherif C, Pooch M, Schulze M, Heuer H, Schiller M, Kupke R and Klein M 2016 Automated detection of yarn orientation in 3D-draped carbon fiber fabrics and preforms from eddy current data *Compos. Part B Eng.* **96** 312–24
- [8] Gao X and Wang L 2015 Finite Element Modelling for Tensile Behaviour of Thermally Bonded Nonwoven Fabric *Autex Res. J.* **15** 48–53